

Physical Characterizations of Ni-Plated Carbon Fibers after Controlled Thermal Treatments

This content has been downloaded from IOPscience. Please scroll down to see the full text.

2009 Jpn. J. Appl. Phys. 48 035503

(<http://iopscience.iop.org/1347-4065/48/3R/035503>)

View [the table of contents for this issue](#), or go to the [journal homepage](#) for more

Download details:

IP Address: 140.113.38.11

This content was downloaded on 25/04/2014 at 11:20

Please note that [terms and conditions apply](#).

Physical Characterizations of Ni-Plated Carbon Fibers after Controlled Thermal Treatments

Chun-Han Lai¹, Guan-Ting Liu¹, Pu-Wei Wu^{1*}, Yu-Fan Chiu¹,
Chao-Ling Chou^{1,2}, and Ching-Jang Lin²

¹Department of Materials Science and Engineering, National Chiao Tung University, Hsinchu 30010, Taiwan, R.O.C.

²Chung-Shan Institute of Science and Technology, Taoyuan 32599, Taiwan, R.O.C.

Received August 20, 2008; accepted December 15, 2008; published online March 23, 2009

Surface modifications of carbon fibers (CFs) were conducted by electroless Ni depositions. After annealing in air at 300 °C, we fabricated a composite in NiO/Ni/CFs configuration. The samples revealed reasonable surface uniformities without defects at the interfaces. Values for the electrical resistivity indicated a steady increase with annealing time, reaching a plateau after 72 h. Results on the tensile stress exhibited a marked reduction once the NiO was formed. A thermal treatment at 700 °C for 48 h in air allowed complete removal of the CFs, forming NiO hollow tubes with an inner diameter of 6.50 μm. Subsequently, they were transformed into Ni hollow tubes with a reduced inner diameter of 5.53 μm under a hydrogen treatment at 400 °C for 3 h. The NiO and Ni tubes demonstrated impressive structural integrities with considerable mechanical strengths. © 2009 The Japan Society of Applied Physics

DOI: 10.1143/JJAP.48.035503

1. Introduction

Carbon fibers (CFs) exhibit unique characteristics in elastic modulus, stiffness, thermal expansion coefficient, corrosion resistance, as well as thermal and electrical conductivities.¹⁾ Hence, they are widely used in a variety of applications as a reinforcement component for composite materials.²⁾ In addition, due to their relatively large surface areas, the CFs have been explored as conductive substrates where metallic nanoparticles are deposited for chemical and biological catalysis.^{3–6)} On the other hand, the CFs could be used as a template to fabricate other functional materials. For example, in electromagnetic interference (EMI) shielding and conductive fabrics, metallic overcoats encapsulating the CFs within are demonstrated.^{7–9)} The metallized CFs are also reported as fillers for gas diffusion electrodes and metal matrix composites.^{10–12)}

Metallization of the CFs has been carried out in several ways. In particular, depositions via the electroless route are known to produce uniform films on conductors and insulators alike.^{13,14)} Among many metals studied for the electroless deposition, the Ni–P chemistry has been studied the most.¹⁵⁾ Recent activities in template synthesis demonstrate nanostructure fabrications by performing electroless Ni depositions on templates such as anodic aluminum oxides and carbon nanotubes.^{16,17)} In some cases, the templates employed are chemically removed to prepare hollow tubes.^{17–19)} Unfortunately, most results reported so far adopt the templates with feature size in submicron ranges. As a result, the nanostructures built upon reveal considerable variations in morphologies and dimensions, which seriously limit their applicability in practical devices. Therefore, the fabrication of hollow tubes in a slightly larger scale attracts substantial interests. In this regard, the CFs are believed to be promising candidates as a suitable template. Previously, Wan *et al.* observed moderate diffusions and dissolutions of Ni in the CFs that contributed to a robust interface between them.²⁰⁾ Moreover, it is understood that the Ni would form a dense and adhering surface oxide preventing further oxidizations. Therefore, we rationalize that the Ni is an appropriate coating material on the CFs, allowing prepara-

tions of composite in NiO/Ni/CFs configuration.

Earlier, we investigated thermal treatments on the CFs coated by Ni, Ag, and Cu, and reported possible formation of oxide tubes.²¹⁾ Our ultimate objective was to prepare cylindrical colloidal crystals by self-assembly of SiO₂ colloids within the hollow tubes for photonic crystal applications. In this paper, we present our results in fabricating Ni-plated CFs and study their electrical and mechanical properties after controlled thermal treatments. In addition, upon complete oxidizations of the CFs, we demonstrate successful formations of NiO and Ni hollow tubes.

2. Experimental Procedure

Electroless depositions of Ni were conducted on the CFs (TORAYCA-T300). The as-received CFs were washed in deionized (DI) water with proper ultrasonication to separate individual CFs. Afterwards, the CFs were cut into lengths of 8.0 cm for subsequent experiments. The electroless depositions involved typical steps of sensitization and activation, followed by Ni reduction and growth. First, the CFs were immersed in a sensitizing solution consisting of 0.3 wt % SnCl₂ and 2.5 wt % HCl. The process lasted for 3 min under ultrasonication to ensure sufficient coverage of Sn²⁺ on the CFs surface. Then, the sensitized CFs were washed in DI water for 30 s, followed by immersion in an activation solution for another 3 min. The formula for the activation solution contained 0.1 wt % PdCl₂ and 1.0 wt % HCl. At this stage, spontaneous oxidation of Sn²⁺ into Sn⁴⁺ induced the reduction of Pd²⁺, forming Pd clusters on the CFs surface. These Pd clusters served as the catalytic centers for subsequent Ni–P depositions. The electrolyte for the electroless deposition included NiSO₄·6H₂O (20 g/L) and NaH₂PO₂ (27 g/L) as the reducing agent. Additives such as Na₂C₃H₂O₄ (19 g/L) and Pb(NO₃)₂ (0.002 g/L) were also employed. Lastly, minute amounts of H₂SO₄ and NaOH were added to adjust the pH of the plating bath to 6.0. The Ni–P depositions were carried out by immersing the Pd-activated CFs in the plating bath at 75 °C for 5 min. Upon sample removal, they were washed in excess water and dried at 60 °C.

For the preparations of composite CFs, we subjected the as-prepared Ni-plated CFs under thermal treatments at

*E-mail address: ppwu@mail.nctu.edu.tw

300 °C in air for various times. Afterwards, they were furnace-cooled slowly to reduce possible thermal damages. The fabrication of NiO hollow tubes was achieved by a heat treatment at 700 °C for 48 h that promoted simultaneously burn-off of the CFs and oxidation of the Ni into NiO. Lastly, the Ni hollow tubes were formed by subjecting the as-prepared NiO hollow tubes in a 99.995% H₂ reducing heat treatment at 400 °C for 3 h.

Field-emission scanning electron microscopy (FE-SEM; JEOL JSM-6700F) was used to observe the morphologies for the Ni-plated CFs. Energy-dispersive X-ray spectroscopy (EDX) was adopted for the composition determinations. Phase identifications were carried out by X-ray diffraction (XRD; Siemens D5000) with a $K\alpha$ of 1.54 Å. Thermal gravimetric analysis (TGA; TA Instruments Q500) was employed to determine the proper temperature for heat treatments. In the TGA analysis, samples less than 3.0 mg were measured with a heating rate of 3 °C/min in a constant air flow of 5.0 cm³/min. The values for the tensile stress of the composite CFs were recorded from a microforce testing system (MTS; Tytron 250). Results on the electrical conductivity were obtained by a four-point probe (Keithley 2000).

3. Results and Discussion

3.1 Electroless deposition and thermal treatments of CFs

Figure 1(a) provides the SEM image for the as-received CFs which exhibited a diameter of 7.0 μm. The image for the Ni-plated CFs is also shown in Fig. 1(b). The thickness for the Ni coating was approximately 470 nm, which corresponds to a deposition rate of 94 nm/min. In addition, the Ni layer appeared rather uniform without notable variations in thickness. Careful observations indicated Ni grains in 400 nm grown perpendicularly from the CFs. As expected, the interface between the deposited Ni and underlying CFs was smooth without voids. This suggests the sensitization and activation steps prior to the electroless deposition were properly conducted, leaving adequate nucleation sites for Ni growths.

The XRD pattern for the Ni-plated CFs is exhibited in Fig. 2. Obviously there appeared a single broad peak at 44° identified as the (111) plane of Ni. Generally, Ni obtained via the electroless route reveals a nanocrystalline nature since the parasitic codeposition of P compromises formation of crystalline phases. This explains the reason for the observed broad diffraction signal. From the EDX data, we confirmed the as-deposited Ni layer with 2 at. % of P.

Figure 3 demonstrates the TGA profiles for the CFs, Ni-plated CFs, and electroless Ni-P film. The Ni-P film was obtained by carrying out the deposition process on a glass slide, followed by careful removal of the Ni-P deposit. In the TGA curve for the CFs, event of noticeable weight loss occurred at 400 °C, indicating the oxidation of C into volatile CO_x was taking place. On the other hand, the TGA response for the Ni-P film showed a negligible weight increase until 500 °C, at which point a rapid weight gain was recorded. The sharp rise in the sample weight suggests considerable Ni oxidation above 500 °C. At 700 °C the oxidation reaction was still unfinished because a complete Ni-NiO transformation amounts to a weight increase of

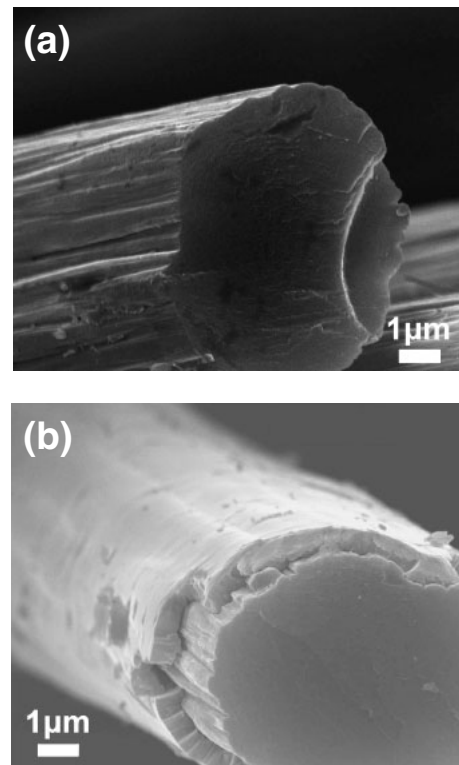


Fig. 1. The SEM images for the (a) as-received CFs and (b) Ni-plated CFs.

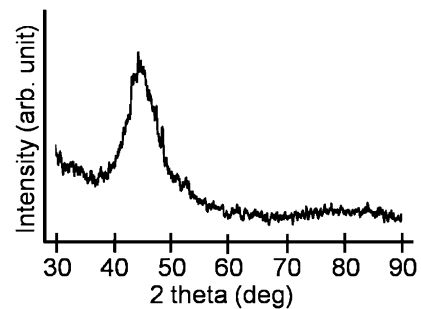


Fig. 2. The XRD pattern for the Ni-plated CFs.

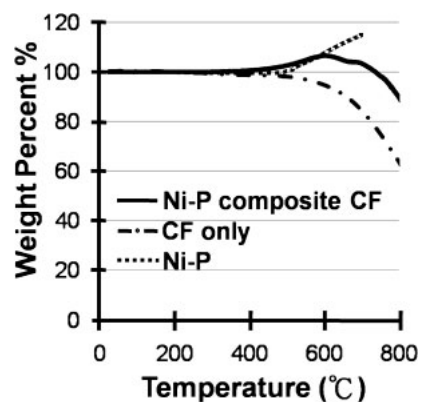


Fig. 3. The TGA profiles for the as-received CFs, Ni-plated CFs, and electroless-deposited Ni-P film.

127%, which is above the measured 115% shown in the curve. In contrast, from the TGA profile of the Ni-plated CFs, we witnessed a slight weight increase around 500 °C,

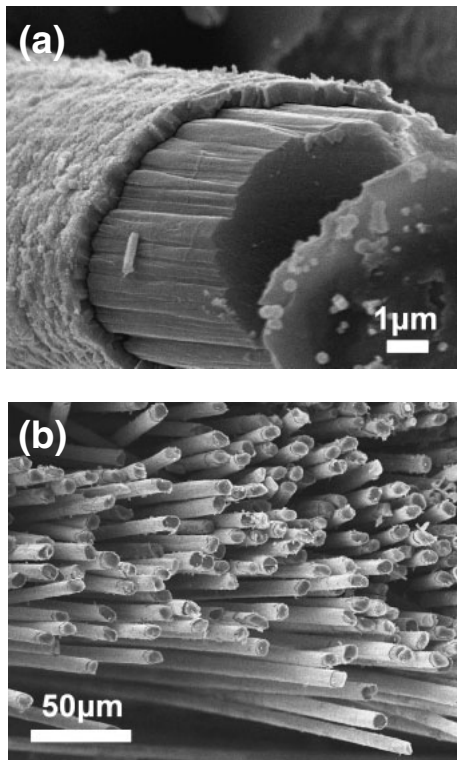


Fig. 4. The SEM images in (a) high magnification and (b) low magnification for the Ni-plated CFs after a heat treatment of 300 °C for 24 h.

corresponding to the oxidization of the Ni layer. However, the weight gain peaked at 540 °C, followed by a gradual weight loss. We rationalized at 540 °C, the oxidation loss of CFs surpassed the weight gain from NiO formation. Judging from the TGA results, we selected 300 °C as the processing temperature to fabricate composite CFs.

Figure 4 presents the SEM images for the Ni-plated CFs after a heat treatment of 24 h at 300 °C. Shown in Fig. 4(a), it can be seen that the Ni layer exhibited a thickness of 530 nm. This amounts to a volume expansion of 119% from the original 470 nm. In principle, the volume expansion for a complete Ni–NiO transformation is expected to be 169%. Therefore, we concluded that the heat treatment for 48 h was inadequate, resulting in composite CFs in NiO/Ni/CFs configuration. Interestingly, the oxidation process rendered negligible de-laminations. This suggests the buried Ni provides sufficient adhesions bonding the NiO and CFs together. A robust interface between the CFs and Ni was confirmed earlier by Shiota and Watanabe.²²⁾ Furthermore, the surface morphologies for the composite CFs became considerably rough because of outgrowth in NiO grains. Figure 4(b) presents the composite CFs in low magnification which suggested the process was reproducible with considerable uniformities among many CFs.

Further EDX analysis using a depth-profiling technique indicated the presence of NiO on the surface. Previously, it was reported that in the oxidation of Ni, out-diffusion of Ni cations dominated over the in-diffusion of O anions.²³⁾ Therefore, formation of NiO occurred at the exterior surface of the oxide film. This not only reduced the internal stress associated with the volume expansion during oxidization but also slowed down the oxidation rate considerably.

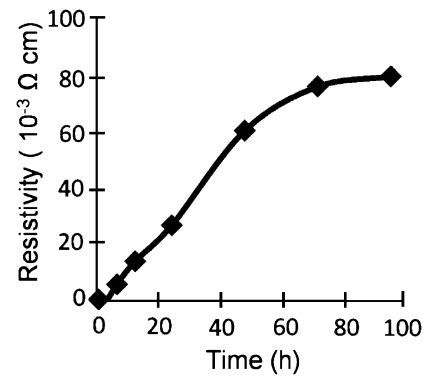


Fig. 5. The effect of heat treatment time on the resistivity of the Ni-plated CFs.

3.2 Physical characterizations

The as-received CFs exhibited a resistivity of $2.04 \times 10^{-3} \Omega \text{ cm}$. In contrast, the resistivity for the as-prepared Ni-plated CFs was $1.34 \times 10^{-4} \Omega \text{ cm}$. The observed reduction for the resistivity is understandable because the Ni is intrinsically more conductive than that of CFs. A simple theoretic calculation following their respective volume ratios in the Ni-plated CFs arrived at $2.95 \times 10^{-5} \Omega \text{ cm}$, a value which is smaller than what we measured. This notable deviation is attributed to the resistivity difference of Ni from metallurgic and electroless routes. In general, the resistivity for a material hinges on several factors including compositions, defects, grain sizes, as well as phases. In our case, the Ni from the electroless deposition existed in a nanocrystalline phase with minute amount of P. As a result, its resistivity value was likely to be substantially larger over that of pure Ni in crystalline phase. Figure 5 provides the values of the electrical resistivity with respect to different processing times. As expected, initial oxidization of Ni formed a resistive NiO on its surface which produced a dramatic rise in the resistivity. As the thermal treatment prolonged, the growth of the NiO was expected to decelerate. This is attributed to the hindered Ni diffusion in the NiO lattice. Further oxidation of the Ni-plated CFs rendered a steady increase of resistivity, reaching a plateau after 72 h. At this stage, the oxidation of the CFs was discontinued as the NiO layer became sufficient thick that limited further Ni oxidization. Careful observations from SEM and XRD determined the surface NiO layer to be 60 nm in thickness.

The evolution for the tensile stress over the thermal treatment times on the composite CFs is demonstrated in Fig. 6. Also provided is the as-received CFs undergoing identical thermal process. The as-received CFs exhibited a tensile stress of 1918 MPa and its values dropped immediately once the treatment was initiated but stabilized after 20 h in the range of 1174–1492 MPa. The substantial reduction in the tensile stress is likely caused by the slow oxidation of CFs that engenders many structural defects. For the as-prepared Ni-plated CFs, the tensile stress was reduced moderately to 1811 MPa from that of as-received CFs. However, the tensile stress was notably decreased once the thermal treatment was applied. At a heat treatment for 12 h, the tensile stress was measured at 498 MPa. Then, there was a steady increase reaching 1142 MPa at 72 h. Afterward, a

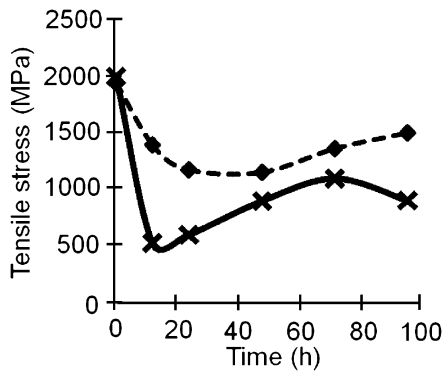


Fig. 6. The effect of heat treatment time on the tensile stress for the as-received CFs (♦) and Ni-plated CFs (x).

further reduction to 924 MPa was recorded at 96 h. This pattern was similar to that of as-received CFs. We surmise that during heat treatments, the conductive Ni overcoat provides an effective thermal conduit to distribute heat uniformly throughout the CFs. As a result, we obtained a stronger oxidation effect for the metallized CFs. In addition, we observed localized damages at the interface between the CFs and Ni from both ends after thermal treatments. These damages possibly served as the defects sites to reduce the tensile stress. Moreover, the expected volume expansion for the Ni oxides provided additional structural inhomogeneity that further reduces the tensile stress. There is another factor to be considered. Once the heat treatment was prolonged, formation of Ni₃P was likely to occur, as suggested by Chen *et al.*²⁴ Hence, the tensile stress was found to increase accordingly. Lastly, SEM observations on the fractured composite CFs indicated a flat surface without debonding, which confirmed the nature of robust interfaces between CFs and Ni.

3.3 Fabrication of NiO and Ni hollow tubes

In addition to the preparation of composite CFs, we investigated further to fabricate NiO and Ni hollow tubes. After extensive explorations in process variables, we determined the proper parameters for desirable tube formations. For NiO hollow tubes, the heat treatment temperature was raised to 700 °C to promote simultaneous oxidation of Ni and CFs. Figure 7(a) presents the images for the NiO tubes with a high magnification picture shown as inset. Apparently, the NiO tubes appeared reasonable strong without breaking into pieces. In addition, the diameter of the hollow core was reduced slightly to 6.5 μm and the thickness of the NiO layer was increased to 750 nm. These variations in diameters are consistent with what we expected. Since a volume expansion of 169% was predicted in the Ni–NiO transformation, the vaporization of CFs permitted moderate changeups in axial direction. In addition, the NiO tubes revealed granular structure evolved from those of as-deposited Ni grains.

A chemical reduction in hydrogen atmosphere was carried out to form Ni hollow tubes. Figure 7(b) provides the nickel tubes with a high magnification picture shown as inset. Substantial volume contraction occurred when the NiO was reduced to Ni. As expected, the diameter for the inner hollow core was reduced further to 5.53 μm, while the thickness for the Ni layer was decreased to 563 nm

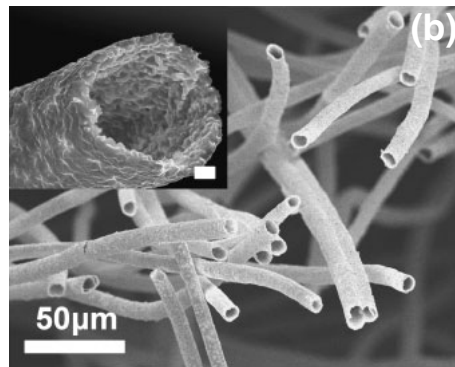
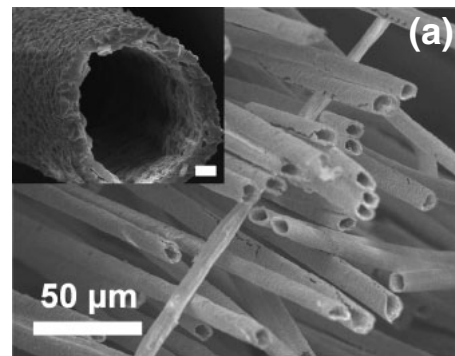


Fig. 7. The SEM images for the (a) NiO hollow tubes and (b) Ni hollow tubes. The insets are the high magnification pictures with the scale bar of 1.0 μm.

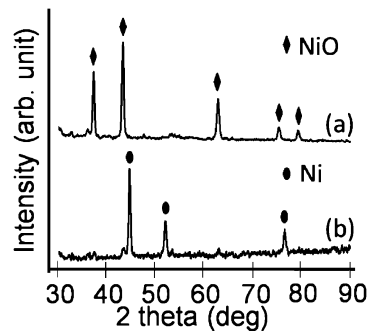


Fig. 8. The XRD patterns for the (a) NiO hollow tubes and (b) Ni hollow tubes.

correspondingly. Notably, the Ni hollow tubes exhibited granular structures suggesting individual grains were properly maintained throughout the process. Moreover, after reversing the treatment steps we were able to convert the Ni hollow tubes back into NiO hollow tubes with impressive structural integrity.

Evidences in XRD patterns confirming the nature of the NiO and Ni hollow tubes are demonstrated in Fig. 8. As shown, we received clear signals indicating phase-pure NiO and Ni were obtained. Previous studies in the microstructural evolutions on the Ni–P films under thermal treatments in vacuum or inert ambient confirmed the formation of Ni₃P in Ni lattice.^{25–27} Notably, the Ni₃P precipitates were not detected after our oxidizing treatments. We suspect the 2 at. % P was evaporating during such a high-temperature heat treatment. We also performed the XRD on grounded powders of NiO and Ni hollow tubes and identical results were obtained.

4. Conclusions

Surface modifications of CFs were conducted by performing electroless Ni deposition on the CFs to form a dense and adhering Ni-P layer. Under heat treatments in air at 300 °C, we fabricated composite CFs in a NiO/Ni/CFs configuration. Evolutions in the tensile stress and electrical resistivity as a function of the heat treatment time were reported. In addition, we annealed the composite CFs at 700 °C for 48 h in air to prepare NiO hollow tubes. Subsequently, they were converted to Ni hollow tubes after a H₂ treatment at 400 °C for 3 h. The composite CFs, as well as NiO and Ni hollow tubes revealed reasonable mechanical strengths and considerable structural integrities.

Acknowledgement

The authors would like to thank the National Science Council of R.O.C. for financial support under the contract of NSC96-2221-E-009-110.

-
- 1) S. Chand: *J. Mater. Sci.* **35** (2000) 1303.
 - 2) K. K. Chawla: *Composite Materials Science and Engineering* (Springer, New York, 1998) p. 252.
 - 3) B. J. Kim and S. J. Park: *J. Colloid Interface Sci.* **325** (2008) 297.
 - 4) S. J. Park and B. J. Kim: *J. Colloid Interface Sci.* **282** (2005) 124.
 - 5) S. J. Park, G. H. Shim, and H. Y. Kim: *J. Colloid Interface Sci.* **291** (2005) 585.
 - 6) B. J. Kim, Y. S. Lee, and S. J. Park: *J. Colloid Interface Sci.* **318** (2008) 530.
 - 7) C. Y. Huang and J. F. Pai: *J. Appl. Polym. Sci.* **63** (1997) 115.
 - 8) X. Gan, Y. Wu, L. Liu, B. Shen, and W. Hu: *J. Alloys Compd.* **455** (2008) 308.
 - 9) J. Jang and S. K. Ryu: *J. Mater. Process. Technol.* **180** (2006) 66.
 - 10) S. Ahn and B. J. Tatarchuk: *J. Appl. Electrochem.* **27** (1997) 9.
 - 11) Y. Tang, L. Liu, Y. Wu, H. Zhan, and W. Hu: *Mater. Lett.* **61** (2007) 1307.
 - 12) X. Wang, Y. Wang, and Z. Jin: *J. Mater. Sci.* **37** (2002) 223.
 - 13) Y. L. Tai and H. Teng: *Chem. Mater.* **16** (2004) 338.
 - 14) M. Hasegawa, N. Yamachika, Y. Shacham-Diamand, Y. Okinaka, and T. Osaka: *Appl. Phys. Lett.* **90** (2007) 101916.
 - 15) M. Schlesinger and M. Paunovic: *Modern Electroplating* (Wiley, New York, 2000) p. 667.
 - 16) S. C. Lin, C. H. Lai, and P. W. Wu: *Electrochem. Solid-State Lett.* **11** (2008) D1.
 - 17) G. Xie, Z. Wang, G. Li, Y. Shi, Z. Cui, and Z. Zhang: *Mater. Lett.* **61** (2007) 2641.
 - 18) S. L. Cheng and W. C. Hsiao: *Electrochem. Solid-State Lett.* **10** (2007) D142.
 - 19) P. Bocchetta, M. Santamaria, and F. Di Quarto: *Electrochem. Solid-State Lett.* **11** (2008) K27.
 - 20) Y. Z. Wan, Y. L. Wang, H. L. Luo, and G. X. Cheng: *J. Mater. Sci.* **36** (2001) 2809.
 - 21) C.-H. Lai, P.-W. Wu, C.-L. Chou, and Y.-F. Chiu: *ECS Trans.* **11** (2008) No. 20, 35.
 - 22) I. Shiota and O. Watanabe: *J. Mater. Sci.* **14** (1979) 699.
 - 23) M. G. Fontana: *Corrosion Engineering* (McGraw-Hill, New York, 1986) p. 505.
 - 24) C. K. Chen, H. M. Feng, H. C. Lin, and M. H. Hon: *Thin Solid Films* **416** (2002) 31.
 - 25) S. S. Tzeng and F. Y. Chang: *Thin Solid Films* **388** (2001) 143.
 - 26) T. Osaka, M. Usuda, I. Koiwa, and H. Sawa: *Jpn. J. Appl. Phys.* **27** (1988) 1885.
 - 27) Q. X. Mai, R. D. Daniels, and H. B. Harpalani: *Thin Solid Films* **166** (1988) 235.